HYDROLOGICAL PROCESSES
Hydrol. Process. (2015)
Published online in Wiley Online Library
(wileyonlinelibrary.com) DOI: 10.1002/hyp.10679

Using concurrent DNA tracer injections to infer glacial flow pathways

Helen E. Dahlke,[1]* Andrew G. Williamson,[2] Christine Georgakakos,[3] Selene Leung,[3] Asha N. Sharma,[3,4] Steve W. Lyon[5] and M. Todd Walter[3]

[1] *Land, Air and Water Resources, University of California Davis, Davis, CA, USA*
[2] *Scott Polar Research Institute, University of Cambridge, Cambridge, UK*
[3] *Department of Biological and Environmental Engineering, Cornell University, Ithaca, NY, USA*
[4] *Charles H. Dyson School of Applied Economics and Management, Cornell University, Ithaca, NY, USA*
[5] *Department of Physical Geography, Stockholm University, Stockholm, Sweden*

Abstract:

Catchment hydrology has become replete with flow pathway characterizations obtained via combinations of physical hydrologic measurements (e.g. streamflow hydrographs) and natural tracer signals (e.g. stable water isotopes and geochemistry). In this study, we explored how our understanding of hydrologic flow pathways can be improved and expanded in both space and time by the simultaneous application of engineered synthetic DNA tracers. In this study, we compared the advective–dispersive transport properties and mass recovery rates of two types of synthetic DNA tracers, one consisting of synthetic DNA strands encapsulated into biodegradable microspheres and another consisting of 'free' DNA, i.e. not encapsulated. The DNA tracers were also compared with a conservative fluorescent dye. All tracers were injected into a small (3.2-km^2) valley glacier, Storglaciären, in northern Sweden. Seven of the nine DNA tracers showed clear recovery during the sampling period and similar peak arrival times and dispersion coefficients as the conservative fluorescent dye. However, recovered DNA tracer mass ranged only from 1% to 66%, while recovered fluorescent dye mass was 99%. Resulting from the cold and opaque subglacial environment provided by the glacier, mass loss associated with microbial activity and photochemical degradation of the DNA is likely negligible, leaving sorption of DNA tracers onto suspended particles and loss of microtracer particles to sediment storage as probable explanations. Despite the difference in mass recovery, the advection and dispersion information derived from the DNA tracer breakthrough curves provided spatially explicit information that allowed inferring a theoretical model of the flow pathways that water takes through the glacier. Copyright © 2015 John Wiley & Sons, Ltd.

KEY WORDS synthetic DNA; tracer; tracer hydrology; glacier; flow pathways

Received 1 February 2015; Accepted 24 August 2015

INTRODUCTION

Identifying sources and flow pathways of water is critical for characterizing the land–stream connections that form the basis of coupled hydrological/ecological/biogeochemical models. Much of our understanding of hydrologic systems has however been based on observations of watershed-integrated signals such as streamflow hydrographs (e.g. Brutsaert and Nieber, 1977; Rupp and Selker, 2005) and tracer responses (e.g. McDonnell, 1990; Burns *et al.*, 1998; McGuire *et al.*, 2007; Dahlke *et al.*, 2014). For example, hydrograph separations using the stable water isotopes (i.e. ^{2}H or ^{18}O) have become a popular analytical approach to derive information on the potential sources and flow pathways of water reaching a stream (see for example the nearly 7000 publications involving deuterium as a hydrologic tracer since 1990; Figure 1). Such tracer experiments have led to increased postulation of hydrologic mechanisms relating the rapid translation of rainfall to runoff (e.g. Bishop *et al.*, 2004; Botter *et al.*, 2010; Klaus *et al.*, 2012). Regardless, the information value of naturally occurring environmental tracers remains rather limited considering the myriad opportunities for water to mix and connect within the landscape (Jensco *et al.*, 2009; Sayama and McDonnell, 2009; Dahlke *et al.*, 2012a; van der Velde *et al.*, 2015).

Application of multiple artificial tracers within one experiment potentially maximizes information gain because it reduces field-experimental efforts (Bösel *et al.*, 2000; Kung *et al.*, 2000; Ptak *et al.*, 2004; Kung *et al.*, 2005) while allowing for direct labelling of multiple water sources or flow pathways. However, the high analytical and laboratory efforts associated with multiple tracers (such as fluorescent, gas, salt tracers; Sr, B, SO_4, O, H

*Correspondence to: Helen E. Dahlke, Land, Air and Water Resources, University of California Davis, Davis, CA, USA.
E-mail: hdahlke@ucdavis.edu

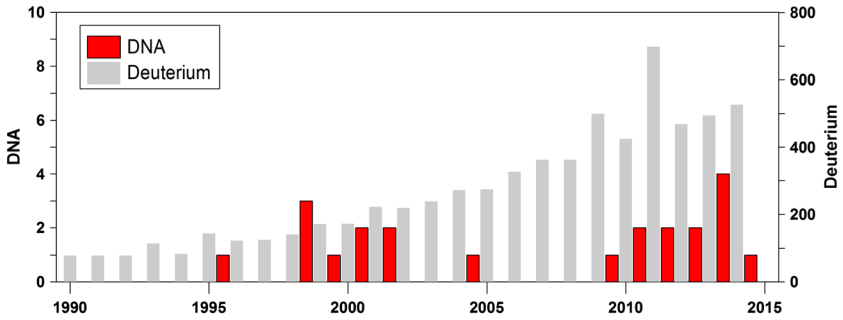

Figure 1. Number of publications since 1990 that have used either deuterium (grey bars) or synthetic DNA in some form (e.g. free DNA or DNA attached to particles or encapsulated by an engineered shell) as a hydrologic tracer. The search was performed using Google Scholar on 10 December 2014

isotopes; and chlorofluorocarbons requiring laboratory technologies ranging from fluorescence spectrometry, wet chemistry, ion chromatography, mass spectrometry to absorption spectroscopy) typically limit the number of different tracers that can be feasibly applied synchronously. Recently, the possibility of performing multitracer applications with a virtually unlimited number of tracers has come into light via the affordable manufacturing of synthetic DNA with individually coded, highly specific (alphanumeric) information (Aleström, 1995).

DNA is a polymer whose building blocks are nucleotides. For tracer experiments, short, single-stranded nucleotide sequences can be designed and produced by automated standard oligonucleotide synthesis (Sabir *et al.*, 1999). Detection and quantification of a targeted DNA sequence are carried out by quantitative or real-time polymerase chain reaction (qPCR). PCR is a laboratory technique that amplifies a small amount of a target DNA sequence into an analytically tractable quantity in a series of thermal cycles in which the DNA is replicated exponentially in an enzymatic process. In qPCR, the amount of DNA produced is monitored at the end of each thermal cycle by measuring the fluorescence of either a non-specific fluorescent dye (e.g. SYBR Green) that binds to double-stranded DNA or a dye that attaches to a predetermined sequence of the target DNA molecule (e.g. Taqman probes). The result is an amplification profile consisting of a sigmoidal graph of the fluorescence as a function of PCR cycle number. The starting amount of the target DNA determines the threshold cycle, Ct, i.e. the cycle number at which the measured fluorescence crosses threshold intensity. PCR is extremely specific, as probes and primers can be designed to anneal to a single, unique DNA target sequence and extremely sensitive, theoretically requiring only a single molecule for amplification (Watson *et al.*, 1992). Further, using single-stranded synthetic DNA molecules provides practically an unlimited number of unique tracers in large quantities (250 nmol or 13.91 g typically consists of 1.5×10^{17} molecules) with essentially identical transport properties for tracing purposes in fluid flow and particulate transport problems.

DNA tracers offer new opportunities to environmental tracer studies, where qualitative and quantitative detection of individual tracers emerging from different sources in the landscape has considerable potential to assist solute transport and flow pathway research. As such, multitracer applications providing space-for-time substitutions could be used to develop new insights into hydrologic systems in the larger landscape context. Until 10 December 2014, only 22 studies have been published since 1990 involving synthetic DNA as a hydrologic tracer (Figure 1). These DNA applications focused mainly on groundwater systems and the comparison of DNA with conservative tracers (e.g. Aleström, 1995; Colleuille and Kitterod, 1998; Sabir *et al.*, 1999, 2000, 2001). Ptak *et al.* (2004) were the first to estimate actual effective transport parameters from DNA tracer breakthrough curves (BTCs) in laboratory experiments and a well-injection experiment. Similar DNA tracer applications in groundwater have been more recently conducted by Palpacelli (2013) and Bovolin *et al.* (2014). In contrast to these studies that applied DNA in its 'free' or unprotected form (i.e. DNA not attached to particles or encapsulated by a protective shell), Mahler *et al.* (1998) tested DNA attached to montmorillonite clay in a laboratory experiment for potential groundwater tracing. Their research showed that unique DNA-labelled particles could be used as a highly sensitive and selective particulate transport tracer while providing some improved stability (i.e. decreased degradation) for the DNA strands. Together, these studies highlight that DNA tracers have a potential to be transported in a manner similar to that of conservative or environmental tracers; however, the exact properties of DNA tracers depend strongly upon the 'type' of DNA tracer applied and the environmental setting of the application (Sharma *et al.*, 2012).

Foppen *et al.* (2011, 2013) and Sharma *et al.* (2012) were the first to test DNA as an applied tracer in surface

water applications. Foppen *et al.* (2011, 2013) compared the breakthrough and recovery rates of six different free DNA tracers and a conservative tracer in several stream channel experiments. Their DNA tracers showed consistent advective–dispersive transport properties, but low mass recovery for the free DNA tracers (3–53%) compared with the conservative tracer (67–106%) (Foppen *et al.*, 2013). Mass loss of the free DNA tracers was attributed to adsorption onto sediment particles, decay and/or biological uptake by microorganisms. Free DNA has been shown to easily adsorb onto clay and other minerals (Greaves and Wilson, 1969; Mahler *et al.*, 1998; Knippers, 2001) whereby adsorption increases with decreasing pH and the presence of divalent cations (Greaves and Wilson, 1969). While free DNA shows some potential as a tracer, it remains unsolved how degradation of the DNA when exposed to ultraviolet (UV) light and/or bacterial activity can be prevented (Pietramellara *et al.*, 2009). These unknown factors currently limit the applicability of free DNA in surface (and to some extent subsurface) water systems.

Since previous experiments have indicated that the longevity of free DNA in the environment can be short, Luo *et al.* (1999a) and Sharma *et al.* (2012) developed short synthetic DNA sequences encapsulated, and thus protected, from the environment and degradation by Food and Drug Administration-approved polylactic acid (PLA) microspheres. The degradation time of these biodegradable PLA microspheres, which have been commonly used in absorbable surgical sutures for over 20 years (Cutright *et al.*, 1971; Craig *et al.*, 1975), is well understood (e.g. Batycky *et al.*, 1997) and can be controlled during fabrication (Cleland and Jones, 1996; Luo *et al.*, 1999a, 2000). Release rates of the material contained within the microspheres have been quantified in laboratory experiments at ~30% in the first few hours, with a gradual decay over several months (Luo *et al.*, 1999b; Smith, 2006). Sharma *et al.* (2012) demonstrated that these engineered DNA microtracers show advective–dispersive properties and recovery rates similar to those observed for conservative tracers (e.g. bromide and blue dye) in column-scale, plot-scale and stream channel-scale experiments.

To field test these novel DNA microtracers at a catchment-relevant scale, we conducted a multitracer experiment on a small (3.2-km^2) valley glacier, Storglaciären, in northern Sweden. This landscape was selected because it offers an isolated system (Dahlke *et al.*, 2014) with fast-flowing conduits (i.e. moulins, crevasses and subglacial channels) relative to the bulk material (i.e. glacial ice). The goal of this field experiment was threefold: (i) to test whether both the free DNA tracers and the microtracers could be recovered in the proglacial streams after passage through the glacier's internal drainage system, (ii) to determine how the recovery of both DNA tracers would compare with that of a conservative tracer, and (iii) to infer the glacier's flow pathways and estimate hydraulic characteristics of the subglacial drainage system.

MATERIALS AND METHODS

Study site

The study was conducted on the 3.2-km^2 sub-polar valley glacier Storglaciären (67°54′N, 18°34′E), in northern Sweden (Figure 2) (Koblet *et al.*, 2010). The glacier is located within the 21.7-km^2 arctic-alpine Tarfala catchment at an altitudinal range of approximately 1130–2100 m above sea level. The valley is characterized by a cold and humid climate with mean annual and summer air temperatures of -3.4 ± 1.0 and 5.9 °C (1965–2009) and a mean annual precipitation of 1997 ± 450 mm (1969–2009) (Dahlke *et al.*, 2012b). Storglaciären has a branched accumulation area (Figure 2) comprising a larger northern cirque and a smaller southern cirque (Jansson, 1996). Glacier ice thickness is variable, ranging between 250 m in the overdeepened upper part of the ablation area and a few metres at the terminus; average ice thickness is 95 m (Jansson, 1996).

The bed topography of Storglaciären has several overdeepened areas (Björnsson, 1981; Eriksson *et al.*, 1993). Above the closure of the largest overdeepening, located approximately 1000 m upglacier of the terminus (Figure 2) (Hooke and Pohjola, 1994), numerous moulins have formed, which feed the majority of the surface meltwater into the glacier (Jansson, 1996). Meltwater that enters the glacier emerges in three major proglacial streams: Nordjokk, Centerjokk and Sydjokk (Figure 2). Nordjokk first appears as an ice-marginal stream upglacier of the terminus on the northern side. Sydjokk comprises two branches, the northern likely forming a confluence with Centerjokk a short distance upglacier of the terminus and the southern emerging upglacier on Storglaciären's southern side before joining the northern branch about 100 m east of the terminus. Both Sydjokk and Centerjokk have high sediment concentrations, indicating substantial subglacial travel (Hock and Hooke, 1993; Hubbard and Glasser, 2005). Most of the subglacial basin's lower third is covered with ~0.2- to 0.7-m-thick glacial till, likely providing the sediment carried by Sydjokk and Centerjokk (Brand *et al.*, 1987; Hooke and Pohjola, 1994). By contrast, Nordjokk is much less turbid, suggesting its discharge is principally englacially derived. Because of their predominant subglacial flow pathways, analysis of water samples for DNA tracer breakthroughs was limited to only Centerjokk and Sydjokk.

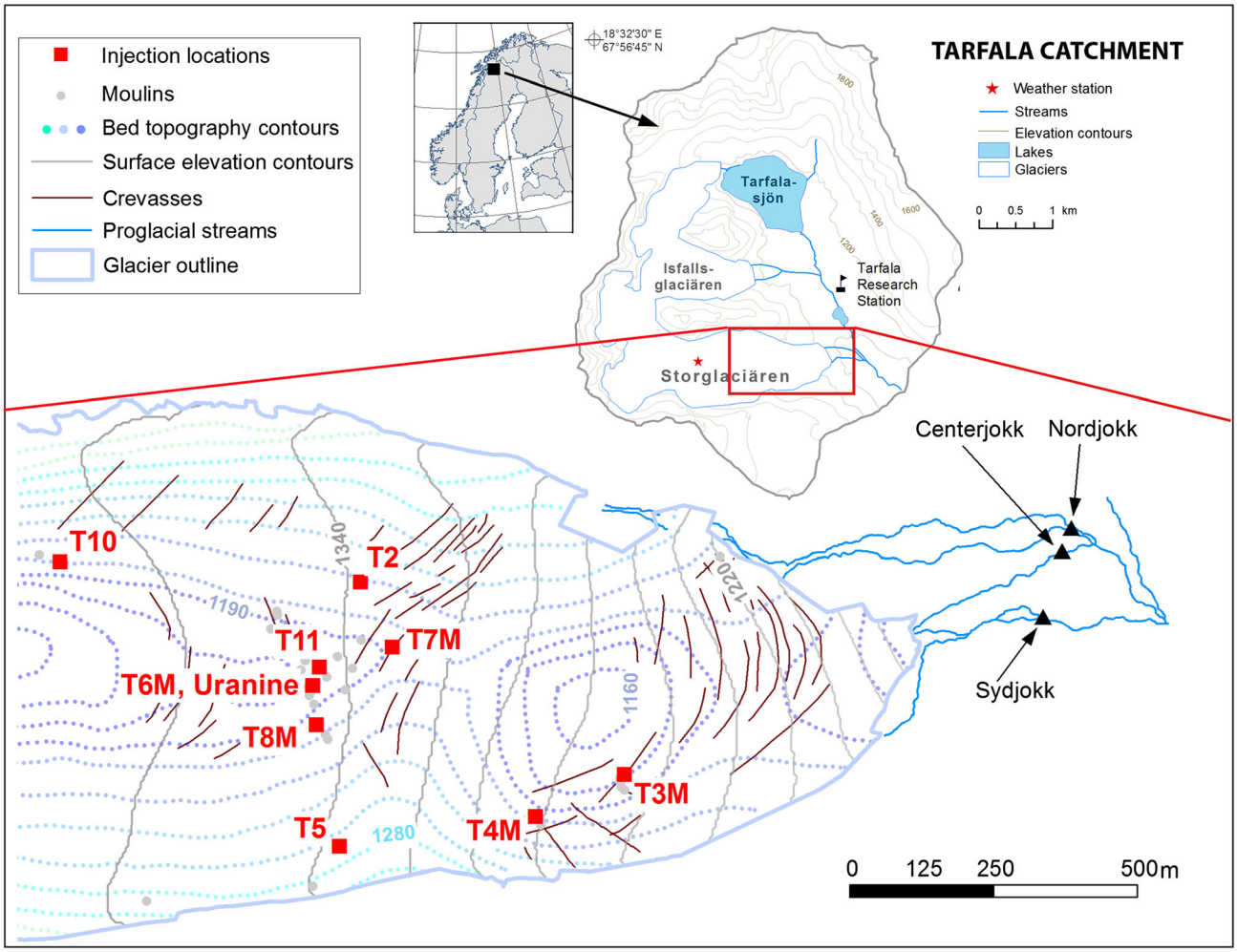

Figure 2. Location and characteristics of the study site, Storglaciären in northern Sweden. The lower map shows the tracer injection locations (squares) and downstream sampling locations (triangles)

Tracer experiment on Storglaciären

Our experiment consisted of simultaneously injecting two types of DNA tracers (free DNA and DNA microtracers) and one conservative fluorescent dye (uranine) into nine locations within the ablation area of Storglaciären in northern Sweden. The DNA tracer experiment was conducted on 5 August 2013 at the end of an unusually warm period (July 23–August 6) when the mean air temperature was 11.9 °C, resulting in a larger meltwater flux into the proglacial streams. Discharge in the two sampled proglacial streams was only measured 30 min prior to and after completion of the experiment using instantaneous fluorescent dye slug injections of 1–2 ml of uranine (33.3% active ingredient) (Hubbard and Glasser, 2005). Discharge was determined based on the uranine BTCs measured either using a calibrated Turner Designs AquaFluor handheld fluorometer/turbidimeter or a GGUN-FL30 fluorometer (Albilia Inc., Switzerland) (Schnegg and Doerfliger, 1997). Average discharges measured prior to and after the DNA tracer injections were 0.95, 1.15 and 0.44 $m^3 s^{-1}$ and 1.03, 1.36 and 0.47 $m^3 s^{-1}$, in Sydjokk, Centerjokk and Nordjokk, respectively.

Preparation of DNA tracers

For the tracer experiments, synthetic DNA for nine different sequences was ordered from IDT DNA (http://www.idtdna.com, Coralville, Iowa, USA) (Table I). First, random 200 base sequences were generated using the freely available GeneDesign Random DNA generator (http://54.235.254.95/cgi-bin/gd/gdRandDNA.cgi, last accessed 24 August 2015). Next, the IDT DNA PrimerQuest Tool (http://www.idtdna.com/Scitools/Applications/Primerquest/) was used to determine an approximate 100-base subsequence for which primers had annealing temperatures between 55 and 60 °C. Total quantities obtained from the synthesis by IDT DNA for each of the nine DNA tracers ranged from 3.3×10^{14} to 2.4×10^{16} particles. The guanine–cytosine content of each

Table I. Nucleotide sequences and assay details of the nine DNA tracers used in this study

	Nucleotide Sequence	Number of bases	Guanine–cytosine content (%)
T2M	5′-G**TGGTGACTACAACAGTGGTGC**AGTGACACCTCG AGCTACGAATGCCCAAGATGTGAGTGCATATCAAG GAGCGGAGCCG**GTTACGACGACCTTATCGGAT**T-3′	102	52.4 (FP), 47.6 (RP)
T3M	5′-AA**AGTAAAGCAGCAGAGGTGGACA**GAGGAAGAG CAGAAGAAGGAAAGAATGCTGGGAAGAGG**AAGAA CGCAAGGCAAAGCGGA**GGTA-3′	87	50 (FP), 52.4 (RP)
T4M	5′-AC**ACGGATCAATCGGATGTCAGGATTC**CCAGCTC GCAACTTACCGACCTGGATGAGGAGTGGCCGTGAA AG**CACAGACACCGTAGAAAAGACAACC**CT-3′	98	48 (FP), 48 (RP)
T5	5′-TC**CTGGGAGTTAGAGTTGGTGGGAATG**ATTCGGT ACGGAGCCGTCGCAGAAGTCGGTAAAACTAAATGG CAA**GGTAGAGCATCTGTAAAAGCCCCTA**GT-3′	99	52 (FP), 48 (RP)
T6M	5′-CC**CAGACTGTCGCTTCATCTGATTGAC**AACATCG GGGCTTGGGAGTCCGGTGGGTAGCTGAGTGA ATGGTG**TCATGTGACAAAGATTCACGGTCTC**TC-3′	98	48 (FP), 44 (RP)
T7M	5′-TC**GCAAGAACTGATTAAAGGCAACCAC**ACTTCCG CAACTCACACGGTTGGTTACAACCGACTTTCCGTGC **CAGCGAGAAAATCTGTTTTGATACGC**CA-3′	98	44 (FP), 42.3 (RP)
T8M	5′-C**CCTAGCGTAGGTCACTTTCATTTTG**TTTCAAGC CACTTCTCTTGCTGGCCGAATACG**CTTTCTTCTAG TCTGTGTCTCTG**T-3′	82	44 (FP), 43.5 (RP)
T10	5′-G**GCTCTCACTGTGTACATGTGTTATC**TGCCTTTC GTCGGGGCGGTAATTCTTGGTGCACAGA**CAATCT TAATAAGAGTCAGGACTGGGT**C-3′	90	44 (FP), 40.7 (RP)
T11	5′-T**CCCTAAGTGTAAGACCTGAGATCGA**CCTGCAG CACACTGACCTCGGAATTACTGCGAAGAGCA**CGT AGAAAGGGGATGTAAGTTAGCC**T-3′	90	48 (FP), 48 (RP)

Bold and underlined letters indicate the forward and reverse primer sequences.

DNA sequence, a measure of the molecule's stability, ranged from 42% to 53%. For each sequence, a Basic Local Alignment Search Tool (BLAST) search was performed using the National Center for Biotechnology Information's Nucleotide Primer-BLAST Tool (http://www.ncbi.nlm.nih.gov/BLAST) (Table I) in order to ensure that the synthetic DNA sequences were not similar to natural DNA sequences.

Microspheres for the microtracers were made using the double-emulsion method (Luo *et al.*, 1999a, b, 2000). PLA of 2000 mg (3001D from NatureWorks LLC, Minnetonka, MN, USA) was dissolved in 20 ml of methylene chloride. Once dissolved, 500 µl of 0.4 µM DNA was added while mixing with a magnetic stir bar; the mixture was cooled and sonicated for a total of 2 min 15 s. Paramagnetic iron oxide nanoparticles were included in the fabrication to facilitate magnetic concentration of the tracers in water samples using the methods of Liu *et al.* (2006). Iron oxide (FeO) of 50 mg is dissolved in 50 ml of nuclease-free water and vortexed briefly to encourage dissolution. Finally, ~40 ml of 1.0% polyvinyl acetate (PVA) was slowly added to the solution after a 15-s sonication round followed by another three rounds of 30-s sonication. The formed emulsion was added to 1000 ml of 0.3% PVA and stirred vigorously for 3 h, cooled, centrifuged, rinsed, frozen at −70 °C and then lyophilized for 24 h to create a powder-like substance. The resultant DNA tracers were stored at 4 °C until further use.

Field measurements

Three free DNA tracers and six DNA microtracers (symbolized by the letter M in the tracer name) were prepared for injection by dispersing the lyophilized DNA mass in approximately 100 ml of purified water. From this suspension, a 1.5-ml sample was pipetted and stored in a sterile 15-ml centrifuge tube to determine the initial tracer mass (C_0) injected at each location on the glacier. The nine different DNA tracers were directly injected into meltwater flowing into eight moulins and one crevasse (location T7M) (Figure 2). In addition, 150 ml of uranine (33.3% active ingredient) was simultaneously injected with a microtracer at location T6M (Figure 2). Injection times ranged from 10:50 to 11:34 hours, local time (GMT+1).

Fluorescent dye concentrations and breakthrough of the DNA tracers were measured at the same locations where discharge was measured on each proglacial stream approximately 226 m (Sydjokk), 313 m (Centerjokk) and 571 m (Nordjokk) downstream of their glacial portals. Instantaneous water samples were collected from all three proglacial streams using sterile 15-ml polystyrene centrifuge tubes. Samples were taken every 5 min for the duration of 3 h after injection of the first tracer. The sampling duration was determined based on uranine injections conducted prior to the DNA tracing experiment, which indicated a time-to-peak concentration of about 60 min. All samples collected during the experiment were stored in an opaque cooler in the field and at 4 °C in a laboratory fridge until further analysis at Cornell University. Breakthrough of the uranine injected at location T6M was determined from the collected stream water samples using a Turner Designs AquaFluor handheld fluorometer (Turner Designs Inc., Sunnyvale, California, USA).

DNA tracer laboratory analysis

DNA concentrations for each synthetic DNA tracer (both the free DNA and the microtracers) were only determined for water samples collected from Sydjokk and Centerjokk as they are the only streams to flow subglacially. Water samples were analysed within 2 months of collection using a Bio-Rad CFX96 Touch real-time PCR system (Bio-Rad, Hercules, CA, USA). For the extraction of the DNA from water samples, we did not utilize the iron oxide nanoparticles but only released the DNA from the PLA microspheres by adding 150−200 µl of methylene chloride to an equal volume of the water sample. The mixture was vortexed briefly and allowed to stand for 10 min. After 10 min of standing, the mixture was centrifuged. The aqueous supernatant containing the DNA was removed using an Eppendorf micropipette and was stored at −20 °C until qPCR was performed. When pipetting the aqueous supernatant, we ensured that the extracted sample was not contaminated with methylene chloride, which is immiscible with water and forms a layer at the bottom of the centrifuge vial. qPCR was performed using SsoAdvanced™ Universal SYBR® Green Supermix (Bio-Rad, Hercules, CA, USA) and a 10-µl total reaction volume per sample, including 5 µl of the SYBR Green Supermix, 0.3 µl each of the forward and reverse primers at a concentration of 25 µM each, 4.4-µl sample and 0.3-µl nuclease-free water. Before carrying out the qPCR analysis on subsamples from tracer release bottles (C_0 samples), each C_0 sample was diluted to reduce the DNA concentration to the limits detected reliably by the instrument. Other samples were not diluted. The serial dilution involved five steps in a tenfold serial dilution series, resulting in a C_0 sample that was 10^5 times diluted compared with its initial concentration. The serial dilution was conducted using an Eppendorf micropipette and sterile, disposable low-retention pipet tips (USA Scientific, Ocala, FL, USA). Latex gloves were worn when handling DNA in the field or laboratory in order to reduce chances of cross-contamination.

The number of DNA particles contained in a water sample was determined using qPCR. Using diethylpyrocarbonate-treated (i.e. DNase/RNase-free) water, a standard curve (Figure 3) was established for each DNA tracer using the Bio-Rad CFX software and the known DNA concentrations for each sequence and by determining the threshold cycle, Ct, for duplicate samples with known concentrations ranging from 0 to 10^7 DNA copies per sample. The standard curve, which is DNA sequence specific, is used to determine the concentration of the targeted DNA sequence in any subsequent water sample from its measured threshold cycle Ct (Table II). Note that the slope of the standard curve has a large influence on the estimated DNA tracer concentrations and tracer recoveries. For this project, we only used the portion of the curve that fit the samples with an $R^2 > 0.99$ and used the lowest point on the curve as the detection limit; e.g. all samples of tracer T4M with fewer than 100 copies were considered non-detectable. For all DNA tracers, the detection limit ranged between 100 and 1000 copies per 4.4-µl sample volume.

Breakthrough curve fitting

In order to compare the performance of the free DNA and microtracers to the conservative fluorescent dye, a one-

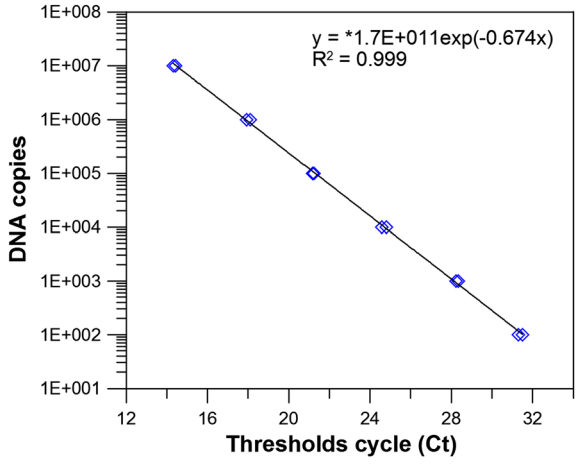

Figure 3. Example of a quantitative PCR (qPCR) standard curve measured for DNA microtracer T4M. The graph is showing the number of DNA copies in the sample *versus* the qPCR cycle number, Ct, at which the threshold fluorescence was reached on the *x*-axis. Standard curve equations and efficiencies for all tracers are listed in Table II

Table II. Molar weight, standard curve equations, standard curve efficiencies and lowest level of detection of the DNA target estimated for each of the nine DNA tracers used in this study

Tracer	Amount ordered (nmol)	Weight (μg)	Lowest level of detection	Standard curve	
			DNA copies	Equation	R^2
T2M	250	15 767.86	1000	$y = 8E+11\exp(-0.743x)$	0.997
T3M	250	13 449.62	100	$y = 1E+10\exp(-0.667x)$	0.999
T4M	250	15 149.89	100	$y = 2E+11\exp(-0.674x)$	0.999
T5	250	15 303.52	1000	$y = 1E+12\exp(-0.772x)$	0.995
T6M	250	15 149.89	1000	$y = 3E+11\exp(-0.643x)$	0.998
T7M	250	15 148.65	1000	$y = 1E+10\exp(-0.577x)$	0.999
T8M	250	12 676.55	1000	$y = 6E+14\exp(-1.103x)$	0.993
T10	250	13 912.97	1000	$y = 6E+10\exp(-0.593x)$	0.998
T11	250	13 913.22	1000	$y = 2E+11\exp(-0.597x)$	0.992

dimensional advection–dispersion equation (ADE) was used to simulate (i) the mean velocity of each tracer through the glacier and (ii) the degree to which each tracer was dispersed during transit, referred to as dispersivity, d (Brugman, 1986; Maloszewski, 1986). Small quantities of the fluorescent dye and the DNA tracers may be lost during transport due to (i) sorption onto sediment, particularly clay (Smart and Laidlaw, 1977; Bencala, 1983, Lorenz and Wackernagel, 1987). In addition, mass loss of the DNA tracers may occur as the result of (ii) DNA degradation by UV light, (iii) consumption by microorganisms and/or (iv) loss of physical stability (mainly affecting free DNA) (Foppen *et al.*, 2011, 2013). Although research shows that glacial environments can have diverse bacterial assemblages (Skidmore *et al.*, 2000; Sigler and Zeyer, 2002) due to the direct injection of the DNA tracer mass into water flowing into the glacier and the rapid passage of the tracers through the glacier, it was assumed that effects (ii) and (iii) were small compared with the potential loss of tracer mass due to adsorption onto sediment. Schneider and Bronge (1996) estimated the suspended-sediment transport from Storglaciären's basin to equal $1.85 \times 10^6\,\mathrm{kg\,km^{-2}\,a^{-1}}$. Because the sediment flux was highly variable during the experiment and turbidity measurements ranged over several orders of magnitude, we included a loss term when fitting the one-dimensional ADE.

Assuming that the longitudinal fluid flow velocity and the dispersion coefficient are constant in time and that accumulation or depletion of the tracer can occur along the flow pathways as a result of the aforementioned processes, the ADE for one-dimensional transport can be expressed as follows:

$$R\frac{\partial C}{\partial t} = D_x\frac{\partial^2 C}{\partial x^2} - u\frac{\partial C}{\partial x} - \mu C + \gamma \tag{1}$$

where u is the longitudinal fluid flow velocity [LT^{-1}], C is the tracer concentration in water (ML^{-3}), D_x is the longitudinal dispersion coefficient accounting for the combined effects of ionic or molecular diffusion and hydrodynamic dispersion [L^2T^{-1}] and x [L] is the longitudinal coordinate. R is the retardation factor describing solute sorption onto sediments, which reduces the apparent advective and dispersive fluxes, μ [T^{-1}] is a first-order decay coefficient or irreversible adsorption coefficient, and γ a zero-order production term [$ML^{-3}T^{-1}$] (van Genuchten *et al.*, 2013).

The dimensionless non-equilibrium two-region (mobile and immobile) transport model is

$$\beta R\frac{\partial C_m}{\partial T} = \frac{1}{P}D_x\frac{\partial^2 C_m}{\partial X^2} - \frac{\partial C_m}{\partial X} - \omega(C_m - C_{im}) - \mu_m C_m \tag{2a}$$

$$(1-\beta)R\frac{\partial C_{im}}{\partial T} = \omega(C_m - C_{im}) - \mu_{im}C_{im} \tag{2b}$$

where C_m and C_{im} are the reduced aqueous concentrations in the mobile and immobile zones, β and ω are the dimensionless mobile water fraction and dimensionless mass transfer coefficient, μ_m and μ_{im} are the decay coefficients, P is the Péclet number ($P = ux/D_x$) and X and T are the dimensionless coordinate and time, respectively (Toride *et al.*, 1995). The longitudinal fluid flow velocity u is estimated from the ratio of x and t_m [T], the time elapsed between injection and peak gauging station concentration (Werder *et al.*, 2010). The velocity, u, should be considered as a minimum flow velocity because channel sinuosity is assumed to be 1 (Seaberg *et al.*, 1988; Hubbard and Glasser, 2005; Sharp, 2005).

In order to infer the morphology of englacial and subglacial drainage pathways, it is common to use the shapes of dye BTCs and quantitative measures derived from BTCs such as the mean transit velocity, dispersivity and tracer recovery (Behrens *et al.*, 1975; Hubbard and Glasser, 2005; Willis *et al.*, 2012). The dispersivity, d [L],

expressing the rate at which the tracer cloud spreads relative to the rate of tracer advection during transit along a flow pathway (Willis *et al.*, 2012) can be estimated as the ratio of the dispersion coefficient, D_x, and the longitudinal fluid flow velocity, u. d-values of approximately 10 or greater indicate travel through highly braided systems and/or easily disrupted channels (Hooke and Pohjola, 1994); lower values (<10) suggest efficient channelized flow (Seaberg *et al.*, 1988; Willis *et al.*, 1990, 2012; Kohler, 1995; Nienow *et al.*, 1998).

Tracer mass recovery, W [M], a measure of the tracer mass that passed the gauging station during each experiment and the amount of dye stored subglacially, was estimated as

$$W = \sum_{t=1}^{n} CQdt \tag{3}$$

where C represents the tracer concentration at time t, Q is the gauging station discharge and dt is the logging interval (Willis *et al.*, 1990, 2012). Because uncertainty associated with the interference of other DNA tracers present in the water sample in the qPCR analysis and the effect of the high turbidity on observed uranine concentrations and dilution of water samples due to pipetting errors could not be quantified, we report uncertainty in mass recovery as one standard deviation of the observed relative concentrations.

The one-dimensional non-equilibrium ADE (Equation (2a)) was solved for each BTC using CXTFIT (Parker and van Genuchten, 1984; Toride *et al.*, 1995; Tang *et al.*, 2010) by fitting d, β and ω with a least squares method and assuming that $\mu = 0$ and $\gamma = 0$. The goodness of fit of each one-dimensional non-equilibrium ADE was estimated by calculating the sum of squared residuals (Tang *et al.*, 2010).

Determining theoretical subglacial drainage system structures

Subglacial flow pathways can be inferred from the bed topography and overlying ice geometry, both of which influence the subglacial water pressure, P_w, of a glacier (Shreve, 1972). If the surface and bed topography of a glacier are known, the subglacial hydraulic potential, Φ, can be estimated using the following equation (adapted from Shreve, 1972):

$$\Phi = \rho_w g z_b + k\rho_i g(z_s - z_b) \tag{4}$$

where ρ_w and ρ_i are water (1000 kg m^{-3}) and ice (917 kg m^{-3}) densities, respectively; g is gravitational acceleration (9.81 m s^{-2}); z_b and z_s are the respective bed and surface elevations (m above sea level); and k is the spatially uniform and non-time-dependent flotation factor, being the ratio of ice-overburden pressure (P_i) to water pressure (P_w) (i.e. P_w/P_i); $k = 1$ indicates subglacial water pressure equals ice-overburden pressure, and $k = 0$ indicates subglacial water pressure equals atmospheric pressure (Shreve, 1972; Rippin *et al.*, 2003; Willis *et al.*, 2012).

Towards producing a theoretical, long-term steady-state structure of Storglaciären's subglacial drainage system, Φ was determined for 11 assumptions of glacier-wide steady-state P_w from atmospheric ($k = 0$) to ice overburden ($k = 1$) at 0.1 increments of k (Williamson, 2013, 2014). Hydraulic-potential grids were calculated from 10-m digital elevation models of the surface (derived from aerial photographs; Koblet *et al.*, 2010) and bed topography (from radio-echo survey point data; Eriksson *et al.*, 1993) of Storglaciären in ArcGIS 10.0 using Equation (4) and following the geographic information system workflow of Willis *et al.* (2012). The likely subglacial drainage system structure (i.e. the locations of subglacial conduits) was determined by comparing, for each P_w assumption, the theoretical and observed locations of ice-marginal and proglacial streams, the emergence of dye returns in proglacial streams to help define the streams' watersheds and the modelled and observed proglacial discharge data (Williamson, 2013).

RESULTS

Tracer breakthrough and mass recovery

The BTCs of all nine DNA tracers and the uranine dye are expressed as relative concentrations of the ratio of observed to initial concentration (C/C_0) *versus* time (Figure 4). All tracers were injected within a 44-min time period at nine locations (Figure 2) with straight-line distances to the proglacial gauging stations ranging from 843 to 1728 and 751 to 1674 m for Centerjokk and Sydjokk, respectively. For each tracer's travel distance, 313 and 226 m were open-channel flow from the glacier terminus to the sampling locations in Centerjokk and Sydjokk, respectively.

Despite the overall noisy BTCs generated for all tracers, uranine (simultaneously injected with microtracer T6M) was detected in both Centerjokk and Sydjokk but not in Nordjokk, supporting the conclusions of previous studies that Centerjokk and Sydjokk are principally responsible for the efficient subglacial drainage of the lower ablation area (Seaberg *et al.*, 1988; Hock and Hooke, 1993). The uranine dye peaked ~57 min after injection (peak $C/C_0 = 16\%$) in Centerjokk and Sydjokk (peak $C/C_0 = 9\%$). The lower uranine concentration observed in Sydjokk is expected because Sydjokk receives water from both the glacial portal (where it splits from Centerjokk) and a secondary channel present near Storglaciären's southern margin.

All of the nine DNA tracers injected were detected in water samples collected from Sydjokk, while only seven

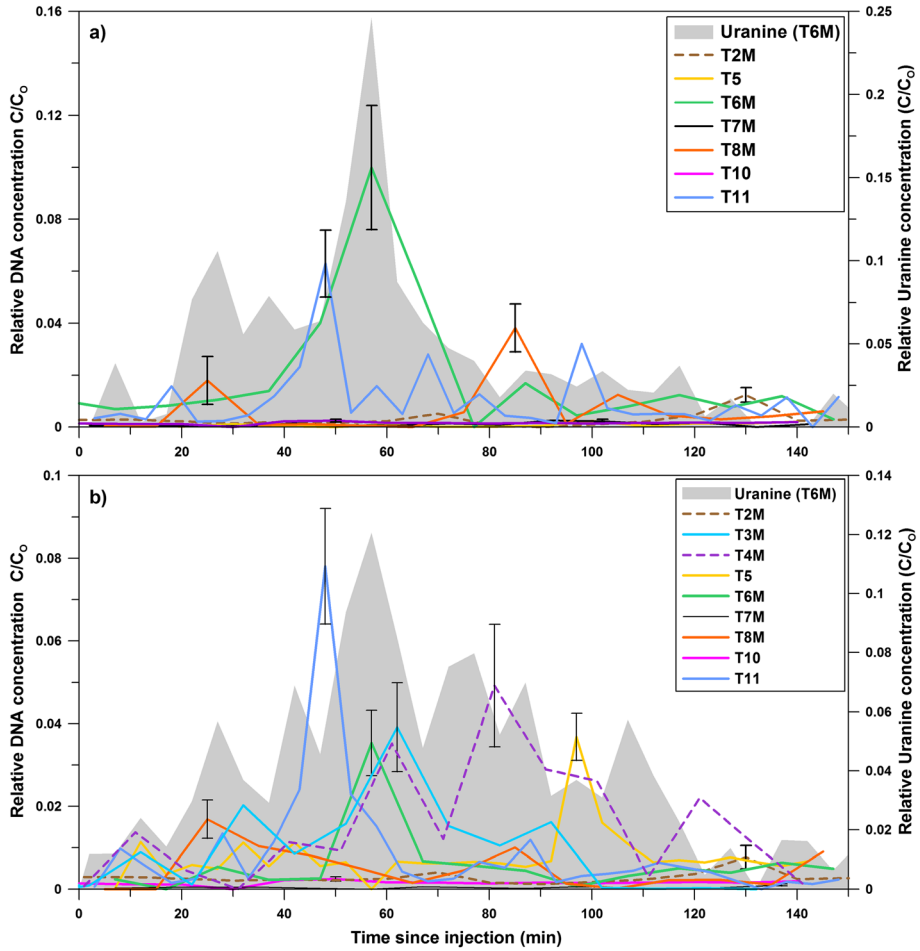

Figure 4. Relative concentration of the uranine fluorescent dye and the nine DNA tracers observed in (a) Centerjokk 313 m downstream of glacial portal and (b) Sydjokk 226 m downstream of glacial portal. Straight-line distances of each injection point to the sampling locations are listed in Table IV. Error bars indicate one standard deviation of the estimated relative concentrations

were detected in water samples collected from Centerjokk. However, of the seven DNA tracers detected in Centerjokk, only four showed obvious peaks in tracer concentration, while in Sydjokk, six of the nine DNA tracers showed significant increases (Figure 4). Among the DNA tracers with clear peaks, T6M showed the highest peak concentration ($C/C_0 = 10\%$) and a 57-min time-to-peak concentration, matching exactly the peak return time observed for the uranine dye. This would suggest that both of these simultaneously injected tracers were transported within the same flow pathways (Figure 4a). The BTC of T8M showed two distinct peaks at 25 ($C/C_0 = 2\%$) and 85 min ($C/C_0 = 4\%$) after injection, which indicates that the tracer cloud was likely split after injection and then transported along two different pathways, either having different lengths or flow velocities. Of the three injected free DNA tracers, T11, injected into a moulin located 35 m north of T6M, showed a 48-min earlier arrival time and the second highest peak concentration ($C/C_0 = 6\%$) of any DNA tracer observed in Centerjokk (Figure 4a).

Three of the nine DNA tracers injected (T6M, T8M and T11) showed significant peaks in both Centerjokk and Sydjokk, with similar peak arrival times but differing peak concentrations. In Sydjokk, T11 peaked 48 min after injection ($C/C_0 = 8\%$), while T6M peaked 57 min after injection ($C/C_0 = 4\%$). Similarly in Centerjokk, T8M peaked twice in Sydjokk at 25 and 85 min after injection, with C/C_0 values of 2% and 1%, respectively. Contrasting with Centerjokk, the water samples from Sydjokk indicated distinct peaks in the BTCs of T3M, T4M and T5, all of which were injected into moulins near the southern margin of the glacier at increasing straight-line distances of 525, 696 and 1033 m from the terminus, respectively. Both microtracers T3M and T4M showed broad or dispersed BTCs relative to other detected breakthroughs, with peaks in Sydjokk showing 62 and 81 min after injection, with C/C_0 values of 4% and 6%, respectively. The free DNA tracer T5 showed a narrower peak 97 min after injection ($C/C_0 = 4\%$). As observed for Centerjokk, T10 and T7M did not show significant concentration increases above background level in

Sydjokk. T7M was the only tracer injected into a crevasse downglacier of the moulin field in the lower ablation area, whereas T10 was injected approximately 400 m further upglacier into a moulin located above the overdeepened area of Storglaciären.

Total mass recovery, estimated as the sum of mass recovered in Centerjokk and Sydjokk, ranged from 1% (T10) to 66% (T6M) for the DNA tracers and 99 ± 7% for the uranine dye (Table III). The high recovery achieved for the fluorescent dye is likely to be due to remobilization of uranine that had been temporarily stored following dye-tracing experiments during the previous day. As is evident from the BTCs, the mass recovery rates of DNA tracers lacking distinct BTCs were small: only 6% (T7M) and 1% (T10), respectively. Recovery rates for DNA tracers T2M, T6M, T8M and T11 in Centerjokk were 8%, 51%, 17% and 32%, respectively. These numbers equal 54%, 77%, 52% and 55% of the total recovered mass for each tracer, indicating that a greater fraction of the bulk tracer mass injected into these locations emerged in Centerjokk rather than in Sydjokk. Total recovery rates for T3M, T4M and T5 were 38%, 46% and 25%, respectively (Table III) and were estimated based on Sydjokk water samples only because of their low detection in Centerjokk.

Comparison of DNA and dye tracer performance

The one-dimensional non-equilibrium ADE was only fitted to BTCs of tracers that showed distinct peaks and recovery rates of more than 15% (Figure 5). Because CXTFIT cannot simulate the split of a single injection into two stream reaches, the observed BTCs in Centerjokk and Sydjokk were considered to be each a stand-alone injection. Because of the noisiness of the data and the rather large temporal increment between observations, achieving convergence of the non-equilibrium ADE in CXTFIT (Equation (2a)) was challenging. The sum of squared residuals (Tang *et al.*, 2010) of all DNA and uranine BTCs ranged between 0.001 and 0.01 (Table IV). In general, dispersivities, dispersion coefficients and mobile water fraction and mass transfer rate coefficients were similar when comparing BTCs of the same tracers in Centerjokk and Sydjokk and when comparing BTCs of the different DNA tracers that emerged in only Sydjokk.

A comparison of the fitted ADEs for the uranine and T6M BTCs showed similar dispersion coefficients of 3.64–5.0 $m^2 s^{-1}$, respectively (Figure 5 and Table IV). Similarly, the BTCs of T11 in Centerjokk and Sydjokk showed similar dispersion coefficients and dispersivities of 0.19 (4.1) $m^2 s^{-1}$ and 0.43 (2.7) m (T11), respectively. The estimated straight-line distance velocities for all

Table III. Total DNA and uranine mass injected and recovered for all simultaneous tracer injections

Tracer	Injection time	DNA mass injected (number of particles)	DNA mass recovered					
			Centerjokk		Sydjokk		Total	
			(number of particles ± SD)	%	(number of particles ± SD)	%	(total number of particles ± SD)	%
T2M	11:15 AM	5.91E+13	4.59E+12 ± 5.32E+10	7.8 ± 0.1	3.96E+12 ± 1.31E+11	6.7 ± 0.2	8.55E+12 ± 1.84E+11	14.5 ± 0.3
T3M	11:23 AM	1.43E+16	n.d.	n.d.	5.42E+15 ± 1.72E+14	37.8 ± 2.1	5.42E+15 ± 1.72E+14	37.8 ± 2.1
T4M	11:34 AM	3.64E+14	n.d.	n.d.	1.68E+14 ± 1.20E+13	46.1 ± 3.3	1.68E+14 ± 1.20E+13	46.1 ± 3.3
T5	11:05 AM	1.59E+16	2.65E+14 ± 1.20E+13	1.7 ± 1.0	3.31E+14 ± 9.40E+12	22.9 ± 0.7	5.96E+14 ± 2.14E+13	24.6 ± 0.7
T6M	10:58 AM	2.40E+16	1.23E+16 ± 5.73E+14	51.4 ± 2.4	3.14E+15 ± 1.90E+14	14.5 ± 0.9	1.55E+16 ± 7.63E+14	65.9 ± 3.3
T7M	11:28 AM	9.91E+14	3.05E+13 ± 7.44E+11	3.1 ± 0.1	2.46E+13 ± 2.41E+11	2.5 ± 0.0	5.50E+13 ± 9.84E+11	5.6 ± 0.1
T8M	10:50 AM	8.33E+15	1.41E+15 ± 7.67E+13	16.9 ± 0.9	1.28E+15 ± 3.99E+13	15.4 ± 0.5	2.68E+15 ± 1.17E+14	32.2 ± 1.4
T10	11:25 AM	3.28E+14	1.04E+13 ± 1.75E+11	0.3 ± 0.1	1.15E+12 ± 1.78E+11	0.4 ± 0.1	2.20E+12 ± 3.53E+11	0.7 ± 0.1
T11	11:07 AM	1.43E+16	4.07E+15 ± 1.58E+14	31.6 ± 1.2	3.33E+15 ± 1.82E+14	25.8 ± 1.4	9.98E+15 ± 1.30E+14	57.4 ± 1.3
Uranine	10:58 AM	4 995 000	3.22E+07 ± 2.82E+07	56.5 ± 3.9	2.13E+07 ± 1.60E+06	42.6 ± 3.2	5.35E+07 ± 2.98E+07	99.1 ± 7.1

Values are provided in total number of particles plus/minus one standard deviation. n.d. indicates that the measured number of DNA particles in the collected water samples was below the quantitative PCR threshold fluorescence (Ct) (Figure 3)

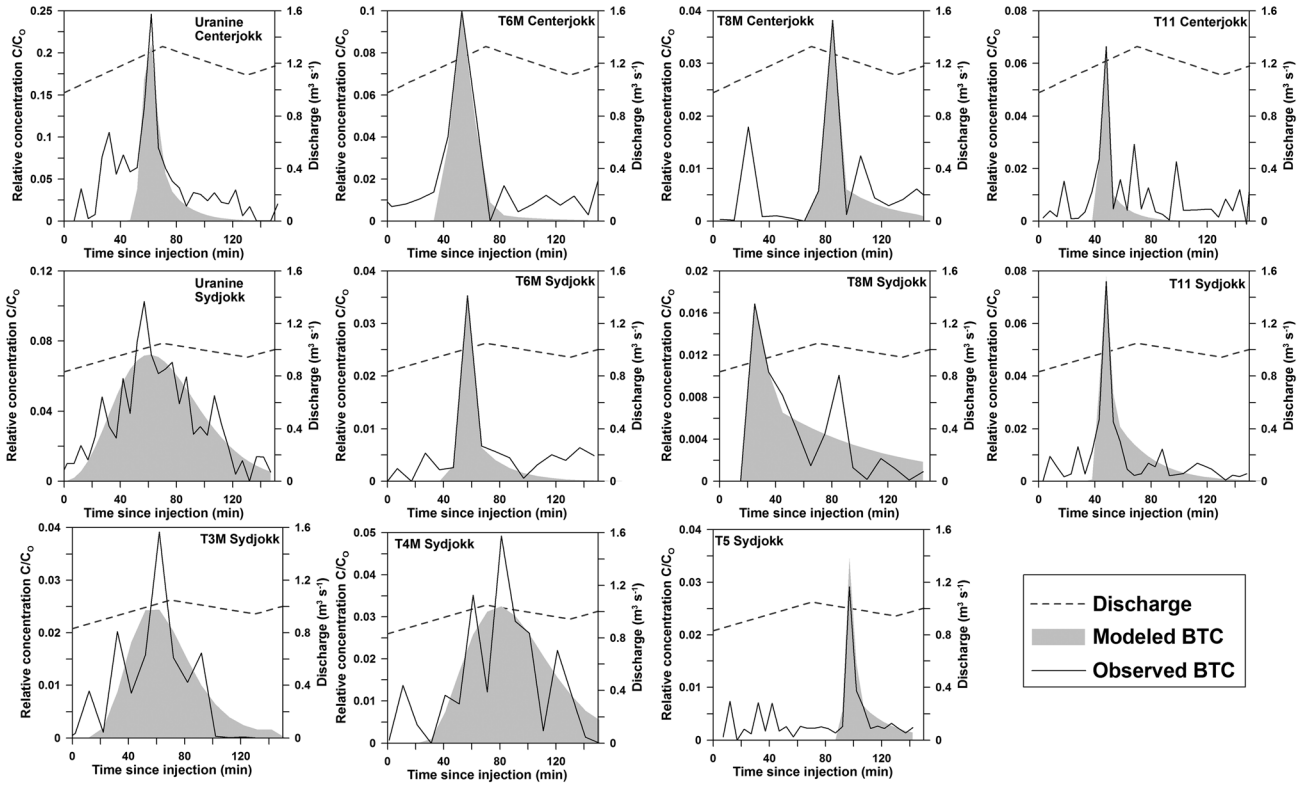

Figure 5. Observed breakthrough curves (BTCs) (lines) and fitted one-dimensional non-equilibrium advection–dispersion equation (filled areas) for selected DNA tracer BTCs and both uranine BTCs, with recovery rates greater than 10%. Dashed lines indicate the discharge measured during the experiment

BTCs ranged between $u = 0.19$ and $0.59\,\mathrm{m\,s^{-1}}$ for both proglacial streams. These velocities are well within the range of previous discharge-velocity observations for Storglaciären (Seaberg *et al.*, 1988; Hock and Hooke, 1993; Kohler, 1995). Although DNA tracers T2M, T6M, T8M and T11 were detected in both Sydjokk and Centerjokk, indicating travel along similar flow pathways, the rather large differences in peak arrival times (Figure 4) and dispersivities despite their similar straight-line travel distances (1206–1318 m) suggest that not all of the injection locations were connected equally well to the same subglacial flow pathways.

Interestingly, despite the variable and increasing distance of injection locations of tracers T3M, T4M and T5 from the glacier terminus, the ADEs fitted for all three DNA tracers showed very similar flow velocities of 0.2, 0.19 and $0.22\,\mathrm{m\,s^{-1}}$ but differing coefficients of dispersion of 5.44, 1.69 and $0.24\,\mathrm{m^2\,s^{-1}}$, respectively, and dispersivities of 22.1, 11.2 and 1.1 m, respectively.

The coefficient of partitioning between the equilibrium and non-equilibrium phases (i.e. mobile water fraction), β, was similar for almost all uranine and DNA tracer BTCs observed in Centerjokk and Sydjokk (0.73–0.94) except for the BTCs of T4M and T8M in Sydjokk, which had $\beta = 0.41$ and $\beta = 0.46$, respectively. The large β values indicate that a relatively small amount of the solute resided in the non-equilibrium or immobile phase. The dimensionless mass transfer rate coefficient (ω) ranged between 0.14 and 0.92 for all uranine and DNA tracer BTCs with two exceptions: the uranine and the T4M BTCs observed in Sydjokk, which converged to rather unrealistically high values of $\omega = 9.98 \pm 188.4$ and $\omega = 6.95 \pm 11.6$, respectively. Most values of the dimensionless mass transfer coefficient were below 0.5, indicating that there was only small diffusion of the tracers into the immobile region as also indicated by the tailing of the modelled BTCs (Figure 5). Although adsorption of the tracers onto sediment particles could not be directly estimated, the shapes of the BTCs fitted with the one-dimensional non-equilibrium ADE (Figure 5) indicate that the adsorption coefficient, K, was rather large because small K-values result in BTCs that are distinctly asymmetric on the rising limb. This is also suggested by the more pronounced tailings of the BTCs that typically occur with increasing values of K (Figure 5) (van Genuchten and Wierenga, 1976).

Inference of the subglacial drainage system structure

Based on the patterns of emergence of the DNA und the uranine tracers, a theoretical reconstruction of the subglacial flow pathways and glacier drainage system

Table IV. IVField-observed and estimated parameter values determined from fitting the one-dimensional non-equilibrium advection-dispersion equation (ADE) to the DNA tracer and uranine dye breakthrough curves (BTCs) using an ordinary least squares method

		Centerjokk							Sydjokk						
Tracer	Injection time	x (m)	u (m s^{-1})	d (m)	β	ω	D_x (m^2 s^{-1})	*SSR*	x (m)	u (m s^{-1})	d (m)	β	ω	D_x (m^2 s^{-1})	*SSR*
T2M	11:15 hours	1206	—	—	—	—	—	—	1150	—	—	—	—	—	—
T3M	11:23 hours	843	—	—	—	—	—	—	751	0.2	27.2 ± 9.55	0.73 ± 0.04	0.14 ± 0.20	5.44	0.01
T4M	11:34 hours	1014	—	—	—	—	—	—	922	0.19	8.91 ± 192	0.41 ± 1.59	6.95 ± 11.6	1.69	0.003
T5	11:05 hours	1345	—	—	—	—	—	—	1259	0.22	0.52 ± 0.06	0.89 ± 0.003	0.71 ± 0.09	0.11	0.001
T6M	10:58 hours	1310	0.38	11.76 ± 2.1	0.94 ± 0.014	0.49 ± 0.09	4.47	0.005	1241	0.36	0.63 ± 0.11	0.94 ± 0.003	0.16 ± 0.05	0.23	0.001
T7M	11:28 hours	1163	—	—	—	—	—	—	1098	—	—	—	—	—	
T8M	10:50 hours	1318	0.56	0.97 ± 0.32	0.86 ± 0.004	0.52 ± 0.14	0.54	0.005	1244	0.59	2.53 ± 0.34	0.46 ± 0.004	0.54 ± 0.08	1.49	0.001
T10	11:25 hours	1728	—	—	—	—	—	—	1674	—	—	—	—	—	—
T11	11:07 hours	1293	0.45	0.43 ± 0.06	0.92 ± 0.001	0.34 ± 0.09	0.19	0.006	1226	0.43	2.66 ± 0.97	0.76 ± 0.01	0.92 ± 0.19	4.12	0.005
Uranine	10:58 hours	1310	0.38	4.76 ± 1.55	0.9 ± 0.016	0.5 ± 0.71	5.02	0.01	1241	0.38	1.031 ± 653	0.001 ± 0.23	9.98 ± 188.4	3.64	0.004

Values of d (dispersivity), β (dimensionless mobile water fraction) and ω (dimensionless mass transfer rate coefficient) are given plus and minus one standard deviation. D_x is the dispersion coefficient estimated as $d^* u$ and SSR is the sum of squared residuals. For DNA tracer T8M, the ADE was only fit to the largest peak. Note that the ADE was only fit to BTCS with recovery rates greater than 15%.

structure can be determined. Of the 11 hydraulic-potential assumptions tested ($k=0$ to $k=1$), the subglacial drainage system structure where $k=0.9$ matched most closely the observed proglacial and ice-marginal stream locations and the observed *versus* modelled patterns of dye-trace returns. This value indicates that 90% of the ice overburden is supported by the subglacial water in this steady-state, long-term configuration. For the $k=0.9$ assumption, Storglaciären is drained by a single major drainage axis, roughly aligned with the glacier centreline (Figure 6). The location of this axis's outlet matches the emergence of Centerjokk and Sydjokk's northern branch from beneath the glacier. For the $k=0.9$ assumption, two minor subglacial axes are present within Storglaciären's lower ablation area, one exiting the glacier on the southern side of the terminus, matching the emergence of Sydjokk's southern branch from beneath Storglaciären, the second matching the location of emergence of Nordjokk. The existence and spatial extent of the southern subglacial drainage axis (i.e. that feeding Sydjokk's southern branch) and watershed are further evidenced by the fact that DNA tracers T5, T4M and T3M, all of which were injected into moulins close to the southern margin of Storglaciären, produced significant breakthroughs only in Sydjokk and not in Centerjokk.

DISCUSSION

On the added value of DNA encapsulation

The glacial environment considered in this study offered a unique opportunity to isolate and compare the free DNA and encapsulated DNA microtracers. As indicated by the BTCs and consistent timing of peaks (Figure 4), the free DNA appears to move in a manner comparable with the encapsulated microtracers. At first consideration, this result holds promise because the processes associated with manufacturing free DNA are significantly lower than those for the encapsulated DNA. However, the cold environment (and slower biological activity than might be present in temperate or tropical climates) and low light exposure (consequently limiting degradation by UV light) found within and beneath the glacier must be accounted for because they offer an almost unique situation. Many surface water environments are not so favourable. As such, the general similarity in mass recovery rates between free DNA and encapsulated microtracers seen in this study may be a product of these favourable conditions and should not be overly generalized.

Considering this almost unique environment, the results suggest that the encapsulated microtracers offer a slight advantage over free DNA as indicated by a lower mass loss observed for the microtracer T6M (66%) *versus*

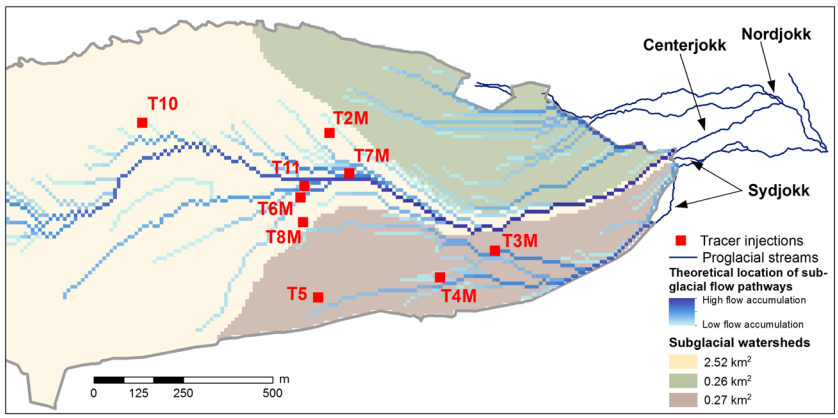

Figure 6. The theoretical subglacial drainage system structure and subglacial watersheds for $k = 0.9$. Observed proglacial streams (dark blue) and injection sites (red) are shown. The theoretical location of subglacial flow pathways is a measure of the number of upstream contributing cells (i.e. the flow accumulation)

the free DNA tracer T11 (57%), both of which were injected into moulins in close proximity to each other (Table III). Again, because we are working within an isolated system that has little (or any) loss to groundwater, revisiting our initial assumption of processes influencing the fate and transport of our DNA tracers along the glacial conduit could provide some insight into the observed differences in recovery rates. Tracer mass loss due to breakdown of the DNA as a result of exposure to UV light is very unlikely because the DNA tracers travelled mainly englacially and subglacially with no exposure to sunlight except for the short open-channel section in the proglacial streams after passage through the glacier. Tracer mass loss due to microbial consumption during the passage through the glacier likely played a smaller role in the recovery as well. Although research has shown that metabolically diverse microbes, including aerobic chemoheterotrophs and anaerobic nitrate reducers, sulfate reducers and methanogens, can be found in glacial environments (e.g. Skidmore *et al.*, 2000; Sigler and Zeyer, 2002), these psychrophilic microorganisms (i.e. organisms adapted to cold environments) have slow growth rates (Morin, 1999; Torsvik and Ovreas, 2008; Schütte *et al.*, 2010). In addition, viable bacteria counts in sediments underneath or in the forefield of glaciers are typically three to four orders of magnitude larger than in glacier ice where counts are often below the detection limit (Foght *et al.*, 2004). Given that the travel time of most DNA tracers through Storglaciären ranged between 40 and 120 min, the loss of DNA due to microbial consumption compared with the loss due to adsorption onto sediment particles or immobile storage is probably very small. However, psychrophilic microorganisms could have a larger effect onto tracer mass loss in sample storage (e.g. storage in the refrigerator at 4 °C).

Sorption of the DNA tracers onto sediment particles, particularly clay (Smart and Laidlaw, 1977; Bencala, 1983; Lorenz and Wackernagel, 1987; Foppen *et al.*, 2011, 2013) and loss of tracer mass to immobile or unconnected storage zones were likely the largest mechanisms by which DNA tracer mass was lost along the glacial conduit(s). The majority of the DNA tracer BTCs had mobile water fraction and mass transfer rate coefficients that indicated relatively small losses or diffusion of the tracer to the immobile phase. However, because of the rather noisy BTCs, the estimated loss coefficients showed a wide range. Nevertheless, the one-dimensional non-equilibrium ADE fitted to the BTCs indicated some differences in the advection and dispersion properties between the microtracers and the free DNA. For example, comparably small dispersivities were found for the free DNA tracers (0.43–2.66 m) and larger dispersivities (0.97–27.2 m) for the DNA microtracers, as indicated by the generally wider BTCs observed for the microtracers. A possible explanation for these differences in dispersivity is that the generally smaller free DNA molecules (<100 nm) are transported more easily than the slightly larger microtracers (average diameter of 480 ± 59 nm; Sharma *et al.*, 2012). In addition, the introduction of paramagnetic iron oxide nanoparticles during the encapsulation process, which adds mass to the microtracer, greatly facilitates our ability to concentrate and analyse the tracer in dilute water samples but might influence transport properties (Sharma *et al.*, 2012). Taken together, there is a justification for using encapsulated microtracers over free DNA. This is particularly true for studies using these tracers in other hydrological systems where conditions may be less favourable than in the glacial environment examined here.

On the advantage of using DNA tracers for flow pathway mapping

The main advantage offered by the microtracers is their ability to label multiple flow pathways (injection points)

simultaneously without concern over confounded or convoluted signals in detection. In this study, simultaneous injection of nine DNA tracers allowed mapping of the principal subglacial drainage system for Storglaciären within a much shorter field effort than would be required using conventional tracers (Figure 6). Comparison of the simulated subglacial drainage network with existing proglacial and ice-marginal stream locations indicated a spatially averaged, steady-state subglacial water pressure of 90% of ice overburden in this study. This result is higher than the value obtained by Williamson (2013) for Storglaciären and that obtained for Midtdalsbreen, Norway, by Willis *et al.* (2012) but compared favourably with the value determined for the Paakitsoq region of the Greenland Ice Sheet by Banwell *et al.* (2013). Lower *k*-values failed to predict Sydjokk's southern branch outlet and the returns of tracers T3M, T4M and T5, which were all injected into moulins along the southern margin of the glacier, in Sydjokk only. The hypothesis that a single principal axis drains Storglaciären's lower ablation area is also corroborated by previous studies (e.g. Seaberg *et al.*, 1988; Hock and Hooke, 1993). Further, the well-defined peaks in conjunction with the high transit velocities ($0.26–0.59\,m\,s^{-1}$), high proglacial discharges ($1–1.2\,m^3\,s^{-1}$) and low dispersivities (0.43–27 m) observed for the DNA tracers BTCs indicate that subglacial flow occurs likely through hydraulically efficient channels. These results are comparable with values observed for channelized, hydraulically efficient systems on glaciers (e.g. Nienow *et al.*, 1998).

Given the highly dynamic nature of glacial drainage systems on timescales ranging from daily (e.g. Schuler *et al.*, 2004; Bartholomew *et al.*, 2010) to seasonal (e.g. Hock and Hooke, 1993; Jobard and Dzikowski, 2006; Bartholomew *et al.*, 2012), 'instantaneous' and potentially repeatable injections of multiple tracers into glacial systems could be deemed crucial for increasing knowledge. Although not considered explicitly in this field experiment where our focus was on the tracer transport behaviour and recovery, our microtracers offer a unique opportunity within glacier hydrology to help resolve the diurnal-to-seasonal evolution of glacier drainage systems at high resolution (e.g. Nienow *et al.*, 1996; Willis *et al.*, 2012; Williamson, 2013). This could be achieved, for example, through repeat labelling of injection points with unique microtracers. Repeating tracer injection after tracer injection is impossible with more traditional tracers (including salt and florescent dyes) because the signals from repeat injections could merge as a result of storage within or slow transit through the glacial system. As our study shows (e.g. for the breakthrough of DNA tracers T10 and T7M; Figure 4), the time for a single tracer to clear the glacier can be considerable and is often longer than one diurnal cycle. With a practically unlimited number of unique tracers, our technology allows collection of a revolutionarily higher quantity of information over short timescales without the worry about uncertainty of whether old or new tracers are being detected.

Moreover, the ability to make multiple injections instantaneously ensures similarity in environmental conditions, which allows increased confidence in subsequent modelling comparisons, especially in the relative sense (whereby the landscape is the first-order control on response; e.g. Lyon and Troch, 2007, 2010). While this is important in any hydrological application, it is paramount in glacial studies because of the inherent temporally dynamic nature of englacial and subglacial drainage pathways, which can change size because of varying water pressures in as little as hours resulting from differences in the glacier's meltwater influx (Hubbard and Nienow, 1997; Schoof, 2010). Moreover, the spatially explicit nature of the microtracers in this study can provide a spatially explicit validation to distributed modelling attempts at characterizing glacial drainage (e.g. Arnold *et al.*, 1998). This spatially explicit nature is deeply needed in hydrology as hydrologists increasingly adopt fully distributed models (e.g. Scanlon *et al.*, 2003; Easton *et al.*, 2007; Kalantari *et al.*, 2014), while still lagging behind with spatially explicit validations (Dahlke *et al.*, 2009; Beven, 2012).

What is next for DNA tracers?

Research involving DNA tracers has made great strides since the early work by Aleström (1995). Of course, there is still room to improve the techniques associated with DNA tracers. Similar to Foppen *et al.* (2011, 2013), we also observed lower mass recovery rates for the DNA tracers compared with the conservative fluorescent dye. Foppen *et al.* (2013) observed a large initial loss of free DNA tracer mass in their small stream experiment and hypothesized that mass loss is influenced by the characteristics of the DNA tracer material and water quality. Based on batch experiments, they ruled out mass loss due to microbial consumption or sorption of DNA onto suspended particles; however, it was hypothesized that the presence of small quantities of trivalent or multivalent cations might cause disintegration of the injected free DNA (Foppen *et al.*, 2013). This indicates that more comparative laboratory and field experiments are needed to provide a better understanding and quantification of the transport, adsorption and degradation processes of synthetic free DNA and microtracers that also systematically investigate the role of soil characteristics and hydrogeochemical conditions on transport properties (e.g. Ptak *et al.*, 2004; Sharma *et al.*, 2012). Although it is known that both the free DNA molecules

and the PLA microspheres (zeta potential −36.7 ±4.3 mV; Smith, 2006) are negatively charged, it would be possible, for example, to fabricate DNA tracers that are physically identical except for the zeta potential, to consequently study sorption effects or reactions with dissolved hydrogeochemicals in the water column. In addition, more research is needed to provide better estimates of how much DNA tracer mass should be injected at a given site to produce DNA concentrations well above the minimum detection limit at downstream sampling locations. For example, low recovery rates were estimated for DNA tracers T2M and T10. Although tracer breakthrough in glacial environments is largely influenced by the connectivity of an injection point to the englacial and subglacial drainage systems (Willis *et al.*, 2012), both tracers had initial injection masses that were two to three orders of magnitude lower than the tracers injected at other locations, which could have contributed to the low detection downstream. Together, these research questions would greatly improve hydrological mass-balance calculations and help establish synthetic DNA tracers as an environmental tracer technology in advection–dispersion transport studies.

CONCLUSIONS

Synthetic DNA tracers consisting of synthetic DNA molecules encapsulated by engineered polymer microspheres can be used to determine advective–dispersive transport processes and to infer the locations and characteristics of flow pathways in glacier hydrologic systems. The two major advantages of synthetic DNA tracers are (i) the availability of a virtually limitless number of unique tracers with essentially identical transport properties and (ii) the extremely sensitive analytical methods available, which theoretically require only a single molecule for detection. In this study, nine different synthetic DNA tracers and one conservative fluorescent dye tracer were simultaneously injected on a small valley glacier, Storglaciären, in northern Sweden to estimate the recoverability of the tracers and to compare the transport properties of DNA tracers at a catchment-relevant scale. Six of the tested DNA tracers consisted of single-stranded DNA molecules encapsulated in engineered polymer microspheres, while three tracers consisted of the synthetic DNA molecules only. DNA tracer concentrations in water samples collected from two proglacial streams were determined through qPCR analysis. From the nine injected DNA tracers, seven, including both free DNA and microtracers, could be recovered within 2 h of injection. Simultaneous injection of one DNA microtracer and uranine fluorescent dye into the same moulin resulted in identical peak arrival times and similar dispersion coefficients, demonstrating that advective and dispersive transport of both tracers was very similar. However, across the experiment, mass recovery was found to be generally lower for the DNA tracers relative to the fluorescent dye, corroborating the presumably initial DNA tracer losses to storage observed in other small-scale surface water applications. Based on the BTCs of the DNA tracers, the subglacial drainage system structure of Storglaciären could be determined, with indication that the subglacial steady-state, glacier-wide water pressure is likely at 90% of ice overburden and that subglacial flow occurred likely in a hydraulically efficient, channelized system during 2013. The results highlight that the application of DNA tracers in favourable environments (e.g. those with slow-growing microbial communities or limited/no exposure to UV light) can be a powerful tool to maximize information gain from a single experiment. The use of synthetic DNA tracers in multitracer applications not only allows direct labelling and tracing of multiple water sources and flow pathways at similar environmental conditions but might also provide spatially explicit information that will help to improve confidence in hydrologic models by facilitating more complex comparisons between simulated and observed hydrological flows.

ACKNOWLEDGEMENTS

We would like to thank Tarfala Research Station for the logistical support of our field experiment. Partial financial support was provided by Stockholm University's trans-national research initiative. In addition, we would like to thank Dr Dan Luo at Cornell University for assistance with the DNA tracer fabrication and laboratory analysis. We would also like to acknowledge funding from the USDA-National Research Initiative (title: Using nano-technology to identify and characterize hydrological flowpaths in agricultural landscapes), NSF (award no. 0853809) and the Heising-Simons Foundation (award no. 2014-59) that allowed us to develop and apply the DNA tracer technology used in this project.

REFERENCES

Aleström P. 1995. Novel method for chemical labelling of objects, International Patent Application PCT/IB95/01144 and Publ. WO 96/17954, World Intel. Prop. Organ. Available at: https://www.google.com/patents/WO1996017954A1?cl=en&dq=Novel+method+for+chemical+labelling+of+objects,+International+Patent+Application&hl=en&sa=X&ved=0CB4Q6AEwAGoVChMIuNPWo7-7TjxwIVCVyICh0seQhZ Last accessed on Sept. 6, 2015.

Arnold N, Richards K, Willis I, Sharp M. 1998. Initial results from a distributed, physically based model of glacier hydrology. *Hydrological Processes* **12**(2): 191–219.

Banwell AF, Willis I, Arnold N. 2013. Modeling subglacial water routing at Paakitsoq, W Greenland. *Journal of Geophysical Research – Earth Surface* **118**: 1282–1295. DOI:10.1002/jgrf.20093.

Bartholomew I, Nienow P, Mair D, Hubbard A, King MA, Sole A. 2010. Seasonal evolution of subglacial drainage and acceleration in a Greenland outlet glacier. *Nature Geoscience* **3**: 408–411.

Bartholomew I, Nienow P, Sole A, Mair D, Cowton T, King MA. 2012. Short-term variability in Greenland Ice Sheet motion forced by time-varying meltwater drainage: implications for the relationship between subglacial drainage system behaviour and ice velocity. *Journal of Geophysical Research* **117**:F03002. DOI:10.1029/2011JF002220.

Batycky RP, Hanes J, Langer R, Edwards DA. 1997. A theoretical model of erosion and macromolecular drug release from biodegrading microspheres. *Journal of Pharmaceutical Sciences* **86**: 1464–1477.

Behrens H, Bergmann H, Moser H, Ambach W, Jochum O. 1975. On the water channels of the internal drainage system of the Hintereisferner, Ötztal Alps, Austria. *Journal of Glaciology* **14**: 375–382.

Bencala KE. 1983. Simulation of solute transport in a mountain pool-and-riffle stream with a kinetic mass transfer model for sorption. *Water Resources Research* **19**: 732–738.

Beven K. 2012. *Rainfall–Runoff Modelling, the Primer*, 2nd edition. John Wiley & Sons, Ltd: West Sussex, England.

Bishop K, Seibert J, Köhler S, Laudon H. 2004. Resolving the double paradox of rapidly mobilized old water with highly variable responses in runoff chemistry. *Hydrological Processes* **18**: 185–189. DOI:10.1002/hyp.5209.

Björnsson H. 1981. Radio-echo sounding maps of Storglaciären, Isfallsglaciaren and Rabots glacier. *Geografiska Annaler* **63A**: 225–231.

Bösel D, Herfort M, Ptak T, Teutsch G. 2000. Design, performance, evaluation and modeling of a natural gradient multitracer transport experiment in a contaminated heterogeneous porous aquifer. *Tracers and Modelling in Hydrogeology* IAHS Publication No. 262 45–51.

Botter G, Bertuzzo E, Rinaldo A. 2010. Transport in the hydrologic response: Travel time distributions, soil moisture dynamics, and the old water paradox. *Water Resources Research* **46**:W03514. DOI:10.1029/2009WR008371.

Bovolin V, Cuomo A, Guida D, Foppen JW. 2014. Using artificial DNA as tracer in a bedrock river of the Middle Bussento Karst System (Cilento, Vallo Diano and Alburni European & Global Geopark, southern Italy). Proceedings of the 7th International Conference on Engineering Mechanics, Structures, Engineering Geology (EMESEG '14), Salerno, Italy, 3–5 June 2014; 105–112.

Brand G, Pohjola V, Hooke RLB. 1987. Existence of a layer of deformable till at the base of Storglaciären, Sweden, revealed by electrical resistivity measurements. *Journal of Glaciology* **33**: 311–314.

Brugman MM. 1986. Water flow at the base of a surging glacier. Ph.D. thesis, Pasadena, California, California Institute of Technology.

Brutsaert W, Nieber JL. 1977. Regionalized drought flow hydrographs from a mature glaciated plateau. *Water Resources Research* **13**: 637–643.

Burns DA, Hooper RP, McDonnell JJ, Freer JE, Kendall C, Beven K. 1998. Base cation concentrations in subsurface flow from a forested hillslope: the role of flushing frequency. *Water Resources Research* **34**: 3535–3544.

Cleland JL, Jones AJ. 1996. Stable formulations of recombinant human growth hormone and interferon-gamma for microencapsulation in biodegradable microspheres. *Pharmaceutical Research* **13**: 1464–1475.

Colleuille H, Kitterod NO. 1998. Forurensning av drikkevannsbronn pa Sundreoya i Al kommune: Resultat av sporstoff-forsok. Norwegian Water Resources and Energy Directorate Report; Oslo, June 1998; in Norwegian.

Craig PH, Williams JA, Davis KW, Magoun AD, Levy AJ, Bogdansky S, Jones JP Jr. 1975. A biologic comparison of polyglactin 910 and polyglycolic acid synthetic absorbable sutures. *Surgery, Gynecology & Obstetrics* **141**: 1–10.

Cutright DE, Beasley JD 3rd, Perez B. 1971. Histologic comparison of polylactic and polyglycolic acid sutures. *Oral Surgery, Oral Medicine, Oral Pathology* **32**: 165–173.

Dahlke H, Lyon SW, Stedinger J, Rosqvist G, Jansson P. 2012b. Contrasting trends in hydrologic extremes for two sub-arctic catchments in northern Sweden – does glacier melt matter? *Hydrology and Earth Systems Sciences* **16**: 2123–2141. DOI:10.5194/hess-16-2123-2012.

Dahlke HE, Easton ZM, Fuka DR, Lyon SW, Steenhuis TS. 2009. Modeling variable source area dynamics in a CEAP watershed. *Ecohydrology* **2**: 337–349.

Dahlke HE, Easton ZM, Lyon SW, Walter MT, Destouni G, Steenhuis TS. 2012a. Dissecting the variable source area concept – subsurface flow pathways and water mixing processes in a hillslope. *Journal of Hydrology* **420-421**: 125–141. DOI:10.1016/j.jhydrol.2011.11.052.

Dahlke HE, Lyon SW, Jansson P, Karlin T, Rosqvist G. 2014. Isotopic investigation of runoff generation in a glacierized catchment in northern Sweden. *Hydrological Processes* **28**: 1383–1398. DOI:10.1002/hyp.9668.

Easton ZM, Gérard-Marchant P, Walter MT, Petrovic AM, Steenhuis TS. 2007. Identifying dissolved phosphorus source areas and predicting transport from an urban watershed using distributed hydrologic modeling. *Water Resources Research* **43**:W11414. DOI:10.1029/2006WR005697.

Eriksson MG, Björnsson H, Herzfeld UC, Holmlund P. 1993. The bottom topography of Storglaciären: a new map based on old and new ice depth measurements, analyzed with geostatistical methods. Forskningsrapportserien STOU-NG 95.

Foght J, Aislabie J, Turner S, Brown CE, Ryburn J, Saul DJ, Lawson W. 2004. Culturable bacteria in subglacial sediments and ice from two Southern Hemisphere glaciers. *Microbial Ecology* **47**: 329–340. DOI:10.1007/s00248-003-1036-5.

Foppen JW, Orup C, Adell R, Poulalion V, Uhlenbrook S. 2011. Using multiple artificial DNA tracers in hydrology. *Hydrological Processes* **25**: 3101–3106.

Foppen JW, Seopa J, Bakobie N, Bogaard T. 2013. Development of a methodology for the application of synthetic DNA in stream tracer injection experiments. *Water Resources Research* **49**: . DOI:10.1002/wrcr.20438.

Greaves MP, Wilson MJ. 1969. The adsorption of nucleic acids by montmorillonite. *Soil Biology and Biochemistry* **1**: 317–323.

Hock R, Hooke RLB. 1993. Evolution of the internal drainage system in the lower part of the ablation area of Storglaciären, Sweden. *Geological Society of America Bulletin* **105**: 537–546.

Hooke RLB, Pohjola VA. 1994. Hydrology of a segment of a glacier situated in an overdeepening, Storglaciären, Sweden. *Journal of Glaciology* **40**: 140–148.

Hubbard B, Glasser N. 2005. *Field Techniques in Glaciology and Glacial Geomorphology*. Wiley: Chichester.

Hubbard B, Nienow P. 1997. Alpine subglacial hydrology. *Quaternary Science Reviews* **16**: 939–955.

Jansson P. 1996. Dynamics and hydrology of a small polythermal glacier. *Geografiska Annaler* **78A**: 169–174.

Jencso KG, McGlynn BL, Gooseff MN, Wondzell SM, Bencala KE, Marshall LA. 2009. Hydrologic connectivity between landscapes and streams: Transferring reach- and plot-scale understanding to the catchment scale. *Water Resources Research* **45**: W04428, DOI:10.1029/2008WR007225.

Jobard S, Dzikowski M. 2006. Evolution of glacial flow and drainage during the ablation season. *Journal of Hydrology* **330**: 663–671.

Kalantari Z, Briel A, Lyon SW, Olofsson B, Folkeson L. 2014. On the utilization of hydrological modelling for road structure design under climate and land use change. *Science of the Total Environment* **475**: 97–103. DOI:10.1016/j.scitotenv.2013.12.114.

Klaus J, Zehe E, Elsner M, Külls C, McDonnell JJ. 2012. Macropore flow of old water revisited: where does the mixing occur at the hillslope scale? *Hydrology and Earth System Science Discussion* **9**: 4333–4380. DOI:10.5194/hessd-9-4333-2012.

Knippers R. 2001. *Molekulare Genetik*. Thieme: Stuttgart.

Koblet T, Gärtner-Roer I, Zemp M, Jansson P, Thee P, Haeberli W, Holmlund P. 2010. Reanalysis of multi-temporal aerial images of Storglaciären, Sweden (1959-99) – part 1: determination of length, area, and volume changes. *The Cryosphere* **4**: 333–343.

Kohler J. 1995. Determining the extent of pressurised flow beneath Storglaciären, Sweden, using results of tracer experiments and measurements of input and output discharge. *Journal of Glaciology* **41**: 217–231.

Kung K-JS, Hanke M, Helling CS, Kladivko EJ, Gish TJ, Steenhuis TS, Jaynes DB. 2005. Quantifying pore-size spectrum of macropore-type preferential pathways. *Soil Science Society of America Journal* **69**: 1196–1208.

Kung K-JS, Kladivko EJ, Gish ET, Steenhuis TS, Bubenzer G, Helling CS. 2000. Quantifying preferential flow by breakthrough. of sequentially applied tracers: silt loam soil. *Soil Science Society of America Journal* **64**: 1296–1304.

Liu X, Kaminski MD, Guan Y, Chen H, Liu H, Rosengart AJ. 2006. Preparation and characterization of hydrophobic superparamagnetic magnetite gel. *Journal of Magnetism and Magnetic Materials* **306**: 248–253.

Lorenz MG, Wackernagel W. 1987. Adsorption of DNA to sand and variable degradation rates of adsorbed DNA. *Applied and Environmental Microbiology* **53**: 2948–2952.

Luo D, Saltzman WM. 2000. Synthetic DNA delivery systems. *Nature Biotechnology* **18**: 33–37.

Luo D, Woodrow-Mumford K, Belcheva N, Saltzman WM. 1999a. DNA controlled release systems using implantable matrices and injectable microspheres. Proceedings of the International Symposium on Controlled Release Bioacting Materials; 1098–1099.

Luo D, Woodrow-Mumford K, Belcheva N, Saltzman WM. 1999b. Controlled DNA delivery systems. *Pharmaceutical Research* **16**: 1300–1308.

Lyon SW, Troch PA. 2007. Hillslope subsurface flow similarity: real-world tests of the hillslope Péclet number. *Water Resources Research* **43**:W07450. DOI:10.1029/2006WR005323.

Lyon SW, Troch PA. 2010. Development and application of a catchment similarity index for subsurface flow. *Water Resources Research* **46**. DOI:10.1029/2009WR008500.

Mahler BJ, Winkler M, Bennett P, Hillis DM. 1998. DNA-labeled clay: a sensitive new method for tracing particle transport. *Geology* **26**: 831–834.

Maloszewski P. 1986. Handbuch zur Anwendung numerischer Fliessmodelle in der Tracerhydrologie. Department of Geography, University of Bern.

McDonnell JJ. 1990. A rationale for old water discharge through macropores in a steep, humid catchment. *Water Resources Research* **26**: 2821–2832.

McGuire KJ, Weiler M, McDonnell JJ. 2007. Integrating tracer experiments with modeling to assess runoff processes and water transit times. *Advances in Water Resources* **30**: 824–837.

Morin PJ. 1999. *Community Ecology*. Blackwell Science, Inc: Malden, MA.

Nienow P, Sharp M, Willis I. 1996. Velocity–discharge relationships derived from dye-tracer experiments in glacial meltwaters: implications for subglacial flow conditions. *Hydrological Processes* **10**: 1411–1426.

Nienow P, Sharp M, Willis I. 1998. Seasonal changes in the morphology of the subglacial drainage system, Haut Glacier d'Arolla, Switzerland. *Earth Surface Processes and Landforms* **23**: 825–843.

Palpacelli S. 2013. Techniques and methodologies for the hydrodynamic characterization of fissured aquifers. PhD Thesis. Doctoral School on Engineering Sciences, Università Politecnica delle Marche, Italy.

Parker JC, Th Van Genuchten M. 1984. Determining transport parameters from laboratory and field tracer experiments. *Bulletin/Virginia Agricultural Experiment Station (USA). no. 84–3.*

Pietramellara G, Ascher J, Borgogni F, Ceccherini MT, Guerri G, Nannipieri P. 2009. Extracellular DNA in soil and sediment: fate and ecological relevance. *Biology and Fertility of Soils* **45**: 219–235.

Ptak T, Piepenbrink M, Martac E. 2004. Tracer tests for the investigation of heterogeneous porous media and stochastic modelling of flow and transport – a review of some recent developments. *Journal of Hydrology* **294**: 122–163.

Rippin D, Willis I, Arnold N, Hodson A, Moore J, Kohler J, Björnsson H. 2003. Changes in geometry and subglacial drainage of Midre Lovénbreen, Svalbard, determined from digital elevation models. *Earth Surface Processes and Landforms* **28**: 273–298.

Rupp DE, Selker JS. 2005. Drainage of a horizontal Boussinesq aquifer with a power law hydraulic conductivity profile. *Water Resources Research* **41**:W11422. DOI:10.1029/2005WR004241.

Sabir I, Aleström P, Haldorsen S. 2001. Use of synthetic DNA as new tracers for tracing groundwater flow and multiple contaminants. *Journal of Applied Sciences* **1**: 233–238. DOI:10.3923/jas.2001.233.238.

Sabir IH, Haldorsen S, Torgersen J, Aleström P, Gaut S, Colleuille H, Pedersen TS, Kitterød N-O. 2000. Synthetic DNA tracers: examples of their application in water related studies, in tracers and modelling in hydrogeology. Proceedings of the TraM 2000 Conference held at Liège, Belgium, May 2000, 159–165, IAHS Publ. 262.

Sabir IH, Torgersen J, Haldorsen S, Aleström P. 1999. DNA tracers with information capacity and high detection sensitivity tested in groundwater studies. *Hydrogeology Journal* **7**: 264–272.

Sayama T, McDonnell JJ. 2009. A new time–space accounting scheme to predict stream water residence time and hydrograph source components at the watershed scale. *Water Resources Research* **45**:W07401. DOI:10.1029/2008WR007549.

Scanlon BR, Mace RE, Barrett ME, Smith B. 2003. Can we simulate regional groundwater flow in a karst system using equivalent porous media models? Case study, Barton Springs Edwards aquifer, USA. *Journal of Hydrology* **276**: 137–158. DOI:10.1016/S0022-1694(03)00064-7.

Schnegg PA, Doerfliger N. 1997. An inexpensive flow-through field fluorometer. 6th Conference on Limestone Hydrology and Fissured Media, La Chaux-de-Fonds, Aug. 1997, 4 pp.

Schneider T, Bronge C. 1996. Suspended sediment transport in the Storglaciären drainage basin. *Geografiska Annaler* **78A**: 155–161.

Schoof C. 2010. Ice-sheet acceleration driven by melt-supply variability. *Nature* **468**: 803–806.

Schütte UME, Abdo Z, Foster J, Ravel J, Bunge J, Solheim B, Forney LJ. 2010. Bacterial diversity in a glacier foreland of the high Arctic. *Molecular Ecology* **19**: 54–66. DOI:10.1111/j.1365-294X.2009.04479.x.

Schuler T, Fischer UH, Gudmundsson GH. 2004. Diurnal variability of subglacial drainage conditions as revealed by tracer experiments. *Journal of Geophysical Research: Earth Surface (2003–2012)* **109**(F2).

Seaberg SZ, Seaberg JZ, Hooke RLB. 1988. Character of the englacial and subglacial drainage system in the lower part of the ablation area of Storglaciären, Sweden, as revealed by dye trace studies. *Journal of Glaciology* **34**: 217–227.

Sharma AN, Luo D, Walter MT. 2012. Hydrological tracers using nanobiotechnology: proof of concept. *Environmental Science & Technology* **46**: 8928–8936. DOI:10.1021/es301561q.

Sharp MJ. 2005. Subglacial drainage. In *Encyclopedia of Hydrological Sciences*, Anderson MG, McDonnell J (eds). Wiley: Chichester.

Shreve RL. 1972. Movement of water in glaciers. *Journal of Glaciology* **11**: 205–214.

Sigler WV, Zeyer J. 2002. Microbial diversity and activity along the forefields of two receding glaciers. *Microbial Ecology* **43**(4): 397–407.

Skidmore ML, Foght JM, Sharp MJ. 2000. Microbial life beneath a high arctic glacier. *Applied Environmental Microbiology* **66**(8): 3214–3220.

Smart PL, Laidlaw IMS. 1977. An evaluation of some fluorescent dyes for water tracing. *Water Resources Research* **13**(1): 15–33.

Smith J. 2006. Colloid transport in porous media: modeling column scale transport with rate constants calculated from pore scale observations. Thesis, Cornell University: Ithaca, NY, August.

Tang G, Mayes MA, Parker JC, Jardine PM. 2010. CXTFIT/Excel – a modular adaptable code for parameter estimation, sensitivity analysis and uncertainty analysis for laboratory or field tracer experiments. *Computers &Geosciences* **36**: 1200–1209.

Toride N, Leij FJ, van Genuchten MTh. 1995. The CXTFIT code for estimating transport parameters from laboratory or field tracer experiments. Version 2.0. U.S. Salinity Laboratory, Agricultural Research Services, U.S. Department of Agriculture, Riverside, CA, 121 pp.

Torsvik V, Ovreas L. 2008. Microbial diversity, life strategies, and adaptation to life in extreme soils. In *Microbiology of Extreme Soils*, Dion P, Nautiyal CS (eds). Springer: Berlin Heidelberg; 15–43.

van der Velde Y, Heidbüchel I, Lyon SW, Nyberg L, Rodhe A, Bishop K, Troch PA. 2015. Consequences of mixing assumptions for time-variable travel time distributions. *Hydrological Processes* **29**: 3460–3474. DOI:10.1002/hyp.10372.

van Genuchten MT, Leij FJ, Skaggs TH, Toride N, Bradford SA, Pontedeiro EM. 2013. Exact analytical solutions for contaminant transport in rivers 1. The equilibrium advection–dispersion equation. *Journal of Hydrology and Hydromechanics* **61**: 146–160. DOI:10.2478/johh-2013-0020.

van Genuchten MT, Wierenga PJ. 1976. Mass transfer studies in sorbing porous media, I, analytical solutions. *Soil Science Society of America Journal* **40**: 473–481.

Watson JD, Gilman M, Witkowski J, Zoller M. 1992. *Recombinant DNA*, 2nd edition. WH Freeman: New York.

Werder MA, Schuler TV, Funk M. 2010. Short term variations of tracer transit speed on Alpine glaciers. *The Cryosphere* **4**: 381–396.

Williamson AG. 2013. The subglacial drainage system structure and morphology of Storglaciären, Sweden. Unpublished B.A. Thesis, University of Cambridge, Cambridge, UK.

Williamson AG. 2014. The hydrological system of Storglaciären, Sweden: integrating modelling with observations. Unpublished M.Phil. Thesis, University of Cambridge, Cambridge, UK.

Willis IC, Fitzsimmons C, Melvold K, Andreassen LM, Giesen RH. 2012. Structure, morphology and water flux of a subglacial drainage system, Midtdalsbreen, Norway. *Hydrological Processes* **26**: 3810–3829.

Willis IC, Sharp MJ, Richards KS. 1990. Configuration of the drainage system of Midtdalsbreen, Norway, as indicated by dye-tracing experiments. *Journal of Glaciology* **36**: 89–101.